

# High Accuracy Gravitational Waveforms from Black Hole Binary Inspirals Using OpenCL

Justin McKennon<sup>\*</sup>  
Electrical & Computer  
Engineering  
University of Massachusetts  
Dartmouth, MA.  
jmckennon@umassd.edu

Gary Forrester<sup>†</sup>  
Physics Department  
University of Massachusetts  
Dartmouth, MA.  
gforrester@umassd.edu

Gaurav Khanna<sup>‡</sup>  
Physics Department  
University of Massachusetts  
Dartmouth, MA.  
gkhanna@umassd.edu

## ABSTRACT

There is a strong need for high-accuracy and efficient modeling of extreme-mass-ratio binary black hole systems because these are strong sources of gravitational waves that would be detected by future observatories. In this article, we present sample results from our Teukolsky EMRI code: a time-domain Teukolsky equation solver (a linear, hyperbolic, partial differential equation solver using finite-differencing), that takes advantage of several mathematical and computational enhancements to efficiently generate long-duration and high-accuracy EMRI waveforms.

We emphasize here the computational advances made in the context of this code. Currently there is considerable interest in making use of many-core processor architectures, such as Nvidia and AMD graphics processing units (GPUs) for scientific computing. Our code uses the Open Computing Language (OpenCL) for taking advantage of the massive parallelism offered by modern GPU architectures. We present the performance of our Teukolsky EMRI code on multiple modern processor architectures and demonstrate the high level of accuracy and performance it is able to achieve. We also present the code's scaling performance on a large supercomputer i.e. NSF's XSEDE resource, *Keeneland*<sup>1</sup>.

## Keywords

OpenCL, GPU, EMRI, Gravity, Relativity

## 1. INTRODUCTION

<sup>\*</sup>Graduate student in the ECE Department.

<sup>†</sup>Graduate student in the Physics Department.

<sup>‡</sup>Associate Professor in the Physics Department.

<sup>1</sup>A 201 TeraFLOP/s, 120-node HP SL390 system with 240 Intel Xeon 5660 CPUs and 360 NVIDIA Fermi M2070 graphics processors, with the nodes connected by an InfiniBand QDR network.

In the near future, a new window onto the universe will be opened. Specifically, the gravitational-wave spectrum that so far has been undetectable, will become observable due to the enormous investment in hardware, theory, and data analysis methods, such as that in the NSF LIGO<sup>2</sup> project (that is undergoing a major upgrade process) and other current and future detectors.

This work is about the calculation of the emitted gravitational waves (GWs) from large and extreme mass-ratio binary inspirals (EMRIs). One of the most promising sources of low-frequency gravitational waves is the capture and inspiral of a compact object (such as a stellar mass black hole or a neutron star) into a supermassive black hole (such as the black holes which exist at the center of many galaxies), following scattering processes in the core of galaxies. Such low frequency gravitational waves are expected to be in the good sensitivity band for space-borne gravitational wave detectors. Studies of the dynamics and the orbital evolution of a binary system in the extreme-mass-ratio limit are therefore an important issue for low-frequency gravitational wave detection.

Theoretical templates of emitted gravitational waves are necessary for detection and for parameter estimation. Typical sources will undergo  $\sim 10^5$  orbits in their last year of inspiral, and it is anticipated that phase coherence of the template with the signal will be required for the entire year for parameter estimation. This requirement drives the need for very long and highly accurate numerical simulations that are able to efficiently generate gravitational waveforms with relative errors lower than  $10^{-4}$ .

In this article we summarize the advances made to our time-domain (TD)<sup>3</sup>, Teukolsky EMRI code [1, 2, 3, 4, 5, 6] that have enabled it to achieve accuracies comparable to those mentioned above, while still maintaining a high degree of efficiency. These advances broadly lie in two distinct categories: *mathematical advances* and *computational performance advances*. In this article, we emphasize the latter and refer the reader to the relevant literature for details on

<sup>2</sup>Laser Interferometer Gravitational-Wave Observatory: <http://www.ligo.caltech.edu/>

<sup>3</sup>As opposed to a frequency-domain approach that works very well in this context; except for cases where there is non-periodicity in the system, such as in the case of a genuine physical inspiral due to a decaying binary system.

the former. More specifically, we present the performance of the TD Teukolsky EMRI code on multiple modern processor architectures (multi-core CPUs and many-core GPUs) using the OpenCL framework and demonstrate the high level of accuracy and performance we are able to achieve. We also present the code's scaling performance on a large supercomputer with GPUs (XSEDE resource: *Keeneland* of Georgia Tech, Oak Ridge National Lab, University of Tennessee-Knoxville and the National Institute for Computational Sciences, funded by the NSF).

## 2. TEUKOLSKY EMRI CODE

Numerical Relativity (NR) is an area of computational science that emphasizes the detailed modeling of strong sources of GWs – collisions of compact astrophysical objects, such as neutron stars and black holes. For the purposes of GW data analysis (detection and parameter estimation), it is critical to have a highly-accurate template bank of theoretical waveforms. Because of the degree of accuracy necessary and the large number of templates required, it is important to develop efficient computational methods for generating these theoretical waveforms. This motivates us to explore parallel computing frameworks like OpenCL and cutting-edge compute hardware like GPUs for NR.

The specific NR application we consider in this work is one that evolves the perturbations of a rotating (Kerr) black hole i.e. solves the Teukolsky equation in the time-domain. In the context of EMRIs, it is the small object that acts as a “source” of the perturbations<sup>4</sup>. In other words, the Teukolsky equation is essentially a linear wave equation in Kerr black hole space-time geometry, with the small object acting as generator of the gravitational waves.

The next two subsections provide more detailed information on this equation and the associated numerical solver code.

### 2.1 Teukolsky Equation

The Teukolsky master equation describes scalar, vector and tensor field perturbations in the space-time of Kerr black holes [7]. In Boyer-Lindquist coordinates, this equation takes the form

$$\begin{aligned} & - \left[ \frac{(r^2 + a^2)^2}{\Delta} - a^2 \sin^2 \theta \right] \partial_{tt} \Psi - \frac{4Mar}{\Delta} \partial_{t\phi} \Psi \\ & - 2s \left[ r - \frac{M(r^2 - a^2)}{\Delta} + ia \cos \theta \right] \partial_t \Psi \\ & + \Delta^{-s} \partial_r (\Delta^{s+1} \partial_r \Psi) + \frac{1}{\sin \theta} \partial_\theta (\sin \theta \partial_\theta \Psi) + \\ & \left[ \frac{1}{\sin^2 \theta} - \frac{a^2}{\Delta} \right] \partial_{\phi\phi} \Psi + 2s \left[ \frac{a(r - M)}{\Delta} + \frac{i \cos \theta}{\sin^2 \theta} \right] \partial_\phi \Psi \\ & - (s^2 \cot^2 \theta - s) \Psi = -4\pi(r^2 + a^2 \cos^2 \theta) T, \end{aligned} \quad (1)$$

where  $M$  is the mass of the black hole,  $a$  its angular momentum per unit mass,  $\Delta = r^2 - 2Mr + a^2$  and  $s$  is the “spin weight” of the field. The  $s = \pm 2$  versions of these equations describe the radiative degrees of freedom of the gravitational field, and thus are the equations of interest

<sup>4</sup>Because of the large mass-ratio, the small companion of a central supermassive black hole can be modeled as a point particle, and the problem can be addressed using perturbation theory.

here. As mentioned previously, this equation is an example of linear, hyperbolic, partial-differential-equations (PDEs) that are quite common in several areas of science and engineering, and can be solved numerically using a variety of finite-difference schemes. The quantity  $T$  in Eq. (1) is the “source” term as mentioned in the previous section. Ref. [7] has a mathematical formula for this quantity and to save space, we will not reproduce that expression here.

### 2.2 Teukolsky Code

To solve Eq. (1) numerically in time-domain we take the approach first introduced by Krivan et al. in Ref. [8]. First, we make use of Kerr spacetime's axisymmetry and factor out the  $\phi$ -dependence of the Eq. (1) by decomposing the solution  $\Psi$  into azimuthal  $m$ -modes

$$\Psi(t, r, \theta, \phi) = \sum_m e^{im\phi} r^3 \Phi_m(t, r, \theta). \quad (2)$$

In this manner the Eq. (1) is reduced to a linear system of decoupled (2+1)-dimensional hyperbolic PDEs. Then, we rewrite this system in first-order form, by introducing a new auxiliary “momentum” field variable,  $\Pi$ . And finally, we develop an explicit time-evolution numerical scheme for this first-order, linear PDE system using the well-known two-step, second-order Lax-Wendroff, finite-difference method. Explicit details on this approach can be found in Ref. [8].

Each iteration to evolve the system above consists of two steps: In the first step, the solution vector  $\mathbf{u} \equiv \{\Phi_R, \Phi_I, \Pi_R, \Pi_I\}$  between grid points is obtained from

$$\begin{aligned} \mathbf{u}_{i+1/2}^{n+1/2} &= \frac{1}{2} (\mathbf{u}_{i+1}^n + \mathbf{u}_i^n) - \\ & \frac{\delta t}{2} \left[ \frac{1}{\delta r^*} \mathbf{D}_{i+1/2}^n (\mathbf{u}_{i+1}^n - \mathbf{u}_i^n) - \mathbf{S}_{i+1/2}^n \right]. \end{aligned} \quad (3)$$

This is used to compute the solution vector at the next time step,

$$\mathbf{u}_i^{n+1} = \mathbf{u}_i^n - \delta t \left[ \frac{1}{\delta r^*} \mathbf{D}_i^{n+1/2} (\mathbf{u}_{i+1/2}^{n+1/2} - \mathbf{u}_{i-1/2}^{n+1/2}) - \mathbf{S}_i^{n+1/2} \right]. \quad (4)$$

The angular subscripts are dropped in the above equation for clarity. All angular derivatives are computed using second-order, centered finite difference expressions. Explicit forms for the matrices  $\mathbf{D}$  and  $\mathbf{S}$  can be easily found in the relevant literature [8].

Symmetries of the spheroidal harmonics are used to determine the angular boundary conditions: For even  $|m|$  modes, we have  $\partial_\theta \Phi = 0$  at  $\theta = 0, \pi$  while  $\Phi = 0$  at  $\theta = 0, \pi$  for modes of odd  $|m|$ . We set  $\Phi$  and  $\Pi$  to zero on the inner and outer radial boundaries.

### 2.3 Mathematical Advances

In this section we enlist the recent mathematical advances that have been made to the Teukolsky EMRI code that play a critical role in it achieving the required level of accuracy and efficiency. The reader is referred to the appropriate literature for details.

1. The TD Teukolsky EMRI code is a (2+1)D, linear, hyperbolic PDE solver that uses a second-order, time-

explicit, finite-difference (two-step Lax-Wendroff) numerical evolution scheme. In the calculations, the smaller member of the binary is viewed as a “source” of perturbations of the black hole that are evolved using the Teukolsky equation, that governs the evolution of perturbations in a Kerr black hole space-time. As a first approximation, one can construe the compact object as being pointlike and structureless. On a discrete spatial grid, a point-like source i.e. a *Dirac delta distribution* can be modeled as a smeared Gaussian distribution. Alternate and more accurate and efficient approaches to modeling a point-like object on a discrete grid have been developed [3, 4]. As an example, one can start by defining a step-function on a discrete numerical grid and then apply the finite-difference derivative operation on the discrete step-function to obtain a “discrete-delta” function on a computational grid. Results based on a refined version of this approach have shown an *order-of-magnitude* improvement in accuracy and efficiency [3, 4].

2. Another recent advance made is due to a *hyperboloidal* compactification for the Teukolsky equation in Kerr space-time. This allows one to include (null) infinity on the numerical grid by attaching a hyperboloidal layer to a compact domain surrounding the rotating black hole and the orbit of an inspiraling point source of GWs. This technique generates gravitational waveforms from large and extreme mass-ratio inspirals in Kerr space-time extracted directly at (null) infinity, while keeping the outer boundary location close i.e. allowing the use of a rather modest sized grid. Tests and comparisons of the results with previous calculations clearly establish the high-level of accuracy and efficiency of this hyperboloidal layer method as applied to our Teukolsky code [6].
3. Higher-order numerical methods have been used very successfully in the context of finite-difference schemes to improve the accuracy of the computations by further reducing the discretization error. However, it is somewhat challenging to create a higher-order convergent numerical-representation of a Dirac delta function and its derivatives and therefore, our code simply performs Richardson extrapolations of its second-order numerical solutions to obtain ones with lower discretization error [3, 4, 5].

## 2.4 Computational Performance Advances

Computational scientists and engineers have begun making use of many-core GPU architectures because these can provide significant gains in the overall performance of many numerical simulations at a relatively low cost. However, to the average computational scientist, these GPUs usually employ a rather unfamiliar and specialized programming model that often requires advanced knowledge of their architecture. In addition, these typically have their own vendor- and platform- specific software development frameworks (SDKs), that are different from the others in significant ways. For example: Nvidia’s GPUs use CUDA SDK [9], AMD’s GPUs use Stream SDK [10], while traditional multi-core processors (from Intel, AMD, IBM) typically employ an OpenMP-based parallel programming model [11].

In 2009, an open standard was proposed by Apple to bring the software development for all these different processor architectures under a single standard – the Open Computing Language (OpenCL) [12] – and all major multi-core processor and GPU vendors (Nvidia, AMD, IBM, Intel) have adopted this standard for their current and future hardware.

In this article, we make use of OpenCL to harness the massive parallelism offered by many-core architectures like GPUs in order to perform high-resolution and long-duration EMRI computations, very efficiently. This plays a critical role in our Teukolsky code’s ability to achieve the required high level of accuracy and efficiency for EMRI simulations. Details are presented later in this article in Section 4.

## 3. OPENCL

As mentioned already, OpenCL is a new framework for programming across a wide variety of computer hardware architectures (CPU, GPU, etc). In essence, OpenCL incorporates the changes necessary to the programming language C, that allow for parallel computing on all these different processor architectures. In addition, it establishes numerical precision requirements to provide mathematical consistency across the different hardware and vendors – a matter that is of significant importance to the scientific computing community. Computational scientists would need to rewrite the performance intensive routines in their codes as OpenCL *kernels* that would be executed on the compute hardware. The OpenCL API provides the programmer various functions from locating the OpenCL enabled hardware on a system to compiling, submitting, queuing and synchronizing the compute kernels on the hardware. Finally, it is the OpenCL runtime that actually executes the kernels and manages the needed data transfers in an efficient manner. As mentioned already, most vendors have released an OpenCL implementation for their own hardware. As of the writing of the document, AMD, Intel and Nvidia have OpenCL freely available for their processors. IBM has also *beta* released OpenCL for their POWER line of multi-core processors.

OpenCL is of tremendous value to the scientific community because it is open, royalty-free and vendor- and platform-neutral. It delivers a high degree of *portability* across all major forms of current and future compute hardware.

## 4. CODE IMPLEMENTATION

In this section we detail our approach taken towards parallelism, not only to take advantage of the many cores of a single GPU, but also those on multiple GPUs. We describe here the different ideas we have implemented and their final performance outcomes [13, 14]. The lessons learned have ultimately helped us converge towards a rather optimal implementation.

The first task in our work is to isolate the most compute intensive portions of our Teukolsky EMRI code. Upon performing a basic profiling of our code using the GNU profiler **gprof**, we learn that computing the “right-hand-sides” of the Lax-Wendroff steps i.e. the quantities within the square-brackets of Eqs. (3) and (4), take most of the application’s overall runtime. We anticipate that this observation is fairly typical for codes of this type. Thus, it is natural to consider

accelerating this “right-hand-side” computation using data-parallelization on the many cores of the GPU.

A data-parallel model is relatively straightforward to implement in a code like ours. We simply perform a domain decomposition of our finite-difference numerical grid and allocate the different parts of the grid to different cores. More specifically, on the GPU, each thread computes the right-hand-side for a *single* pair of  $r$  and  $\theta$  grid values. In addition, it is necessary to establish the appropriate data communication between the GPU cores and the remaining code that is executing on the CPU – we use `clEnqueueReadBuffer`, `clEnqueueWriteBuffer` instructions to transfer data back-and-forth from main memory and we only use *global memory* on the GPU to simplify communication between the GPU cores. We make this simplification with the goal of keeping the code’s *portability* intact, even if it impacts performance to some extent [14].

Unfortunately, this naive approach yields a *negligible* performance gain on the GPU. The reason is that although the right-hand-side computation is accelerated due to the use of the many-cores of the GPU, the time it takes to bring that data back-and-forth from main memory so that the remaining computation can resume on the CPU, is large enough that no overall gain in performance is perceived. This outcome is simply due to the limited bandwidth of the system’s PCI bus on which the GPU is located. To address this issue, we port *all* the Lax-Wendroff related compute routines (such as the computation of the evolved fields half-way between grid points, the boundary condition imposition, updating of the fields using the right-hand-side data) as separate kernels onto the GPU. In this manner, no communication is necessary with the rest of the computer system and we overcome the challenge mentioned above. It is worth noting that some of these routines are perhaps not ideal for execution on the GPU (for example, some don’t quite have a high enough *arithmetic intensity* that is essential to obtain high performance from the GPU architecture) but we still port these over for execution on the GPU regardless, simply because our goal is to minimize data transfer back-and-forth from main memory. This requires a significant amount of additional effort – but one that pays off well eventually (as seen in the following section).

Porting the source-term computation i.e. the expression for  $T$  onto the GPU using OpenCL was particularly challenging. The reason is that this expression *requires* complex number algebra support and because OpenCL kernels do not currently support C++ features, we could not simply use equivalent user-defined datatypes and operations using *operator overloading*. In operator overloading, the user specifies the operation of the mathematical operators by specifying the behavior of the operator on the user defined datatypes. In this light, mathematical operators are simply function calls, and the left and right hand side of each operator act as the arguments to these functions. Through a transformation from this standard *infix* notation to *prefix* notation, the operator can be forced to precede its arguments without losing the order of operations, thus forcing the mathematical function calls to closely mimic that of standard C-style function calls. From this point, the operators can be replaced by C-struct function calls by way of a recursive find and replace

search tree algorithm. In this manner, complex arithmetic can be realized by having the C-struct functions return a struct with both real and imaginary components, preserving the integrity of the source-term expression.

The main limitation that we introduce with this approach of running the entire computation on the GPU is that we need to be able to fit the entire memory requirements of the code within the GPU video memory. Given that current high-end GPU offerings support only a few GBs of memory, this can be challenging. However, a compute cluster with multiple GPUs per node, such as NSF’s XSEDE *Keeneland*, can overcome this serious limitation.

Another distinct approach to code parallelism that we attempted involves leaving the source-term  $T$  computation on the multiple CPU cores and performing the rest on the many cores of the GPU. This has several advantages. First, we have full support for complex datatype on the CPU from standard math libraries. Second, we can make effective use of the powerful CPU cores during the computation, instead of leaving them mostly idle. Given the nature of the “discrete-delta” i.e. being non-zero on only a handful of grid points and the computational complexity of the source-term [13], that portion of the calculation is actually *better* suited for the few “sophisticated” CPU cores, as opposed to the many “simple” GPU cores. And finally, only a rather modest amount of data needs to be exchanged over the PCI bus, again, because the source-term is non-zero on a small number of grid points. Through detailed experimentation, we realized that this approach is quite optimal for our code and therefore, this is the final approach towards parallelism that we moved forward with.

It is worth mentioning that we did not make a serious attempt to hand-tune the codes to tailor them for each architecture, in order to obtain maximal performance. As stated earlier, one of our goals is to keep the code highly portable, because we aim to run the exact same code on both GPUs and CPUs. The only variable that we tuned (through simple experimentation) in order to obtain maximum performance for each architecture is the value of the *local workgroup size*. Developing the OpenCL kernels themselves did not require much restructuring of the original routines. Most of the effort was spent in the separating out what computation executes on the GPU/CPU and then setting up the communication and synchronization between them. Overall, it took the equivalent of two full-time (beginning) engineering graduate students working for a year to completely develop, test and benchmark this OpenCL code.

Finally, to extend our parallel approach to multiple GPUs we considered the standard domain-decomposition approach using message-passing (MPI). However, we discovered<sup>5</sup> a novel and simpler alternative i.e. a “temporal” parallelization approach, instead of a spatial one (like domain-decomposition). Such a technique relies on the fact that our code is solving a linear problem, and that the trajectory for the inspiraling object is generated separately [4, 5]. In addition, we are only interested in the “quasi steady-state” part of the solution (recall that code has a “forcing” source-term). Given

<sup>5</sup>We thank Pranesh Sundararajan for suggesting this approach.

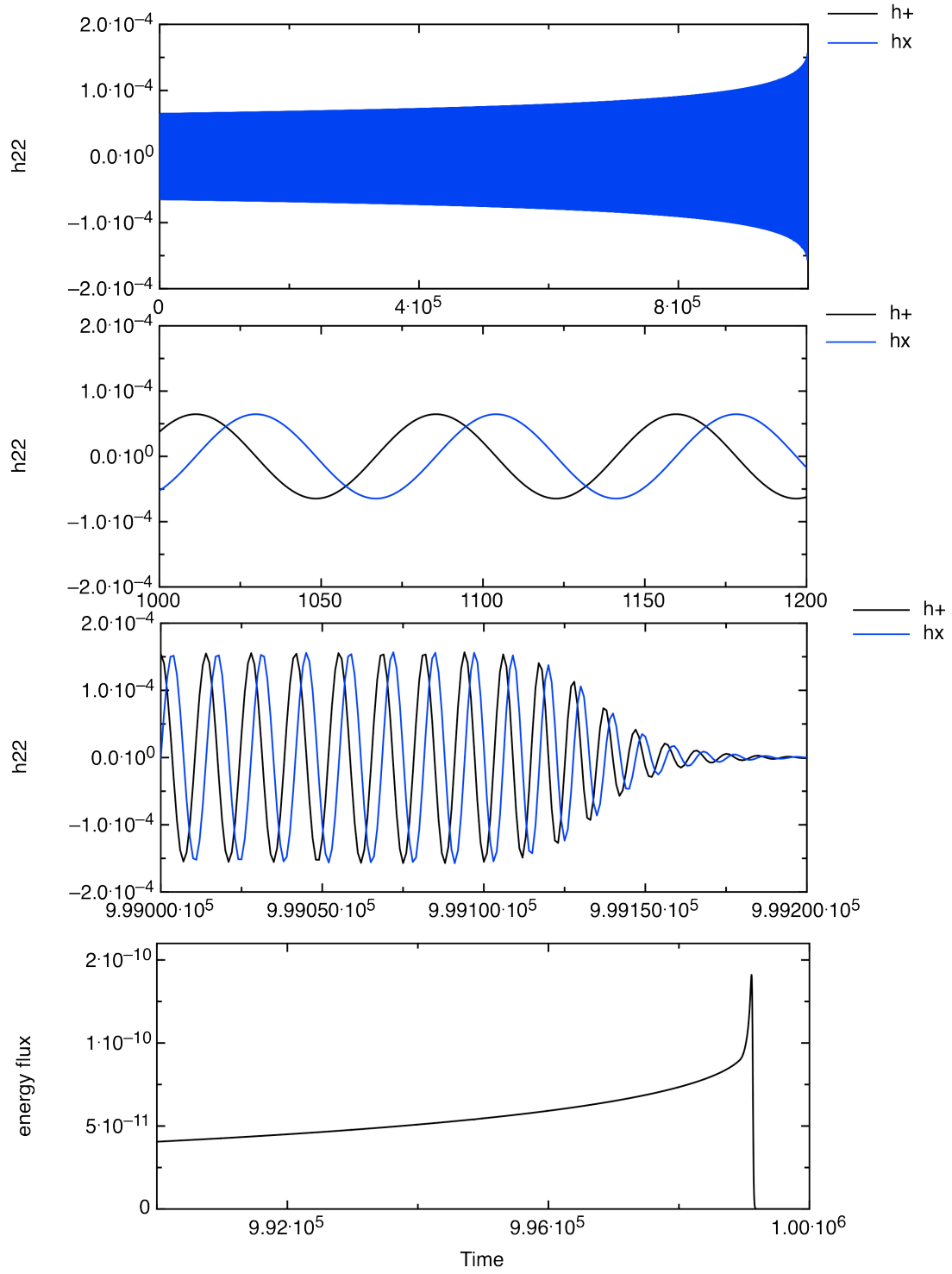


**Figure 1: A complete EMRI gravitational waveform ( $h_{22}$ ) generated using our time-domain Teukolsky EMRI code.**

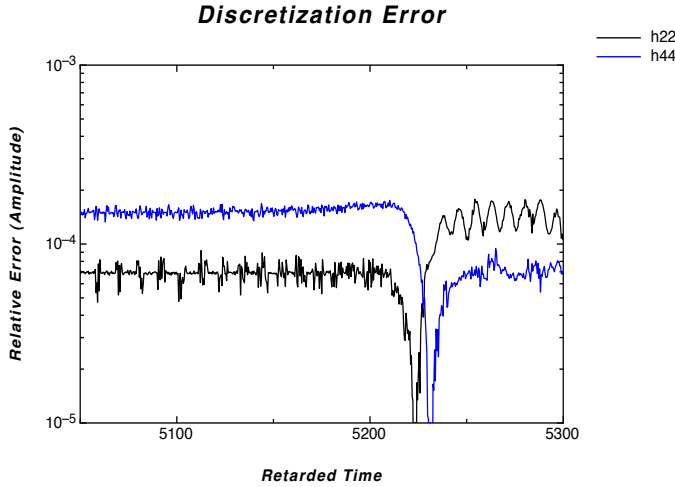


**Figure 2:** Relative errors in the amplitude of the  $h_{22}$  and  $h_{44}$  modes of the gravitational waveform. Compare with Figure 1 in Ref. [16].

these facts, it is possible to split the trajectory into several equal and short time-segments and then perform the short time-evolutions for generating the gravitational waveforms from each segment, in parallel. Then as a final step, we can “patch” these short waveforms together into a complete long waveform. There were some challenges along the way, such as handling the “junk” radiation burst in each of these short time-evolutions but there are known techniques to minimize the effect of these artifacts [22]. This approach is particularly promising for *strong* scaling of our code on large parallel systems because it nearly eliminates all the communication necessary between different compute nodes. We present the scaling outcome from this approach in the next section.

## 5. RESULTS

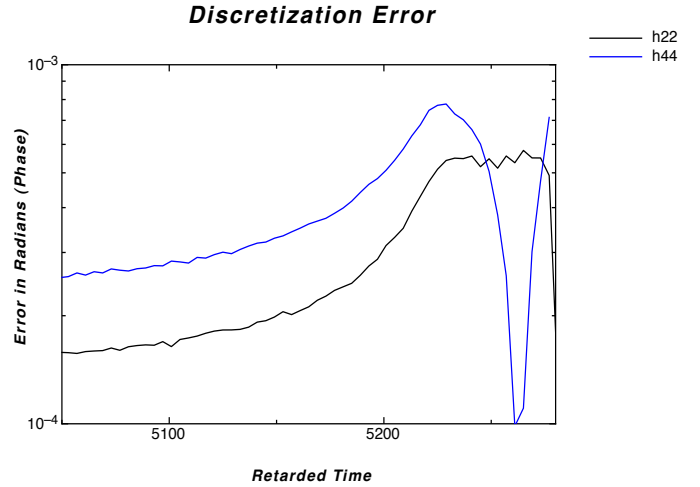
This section is dedicated to the outcomes from the mathematical and computational advances made to our Teukolsky EMRI code detailed in the previous sections.

Figure 1 presents a complete EMRI gravitational waveform generated using our time-domain Teukolsky EMRI code. The mass-ratio used for this evolution is  $10^{-4}$  and the (circular, equatorial) orbital decay covers all phases, from the adiabatic inspiral to the plunge regime. The duration of the inspiral is a *million*  $M$  long i.e. over 10,000 full orbital cycles. The data shown in the plot is the  $\ell = m = 2$  “spin-weighted” spherical harmonic projection of the full gravitational wave strain i.e.  $h_{22}$ .

### 5.1 Accuracy

In Figures 2 and 3 we depict the discretization errors from a sample high-accuracy computation<sup>6</sup>. It is clear that for the most part the errors stay at acceptably low levels (on the scale of  $10^{-4}$ ). However, towards the tail end of the computation, the errors do grow to somewhat higher lev-

<sup>6</sup> This error estimate is obtained by computing the waveform data’s Richardson extrapolant two different ways and then taking the relative difference between these two. The highest  $(r, \theta)$  resolution in use here is  $(M/320, \pi/200)$ .



**Figure 3:** Error in the phase of the  $h_{22}$  and  $h_{44}$  modes of the gravitational waveform. Compare with Figure 1 in Ref. [16].

els. This happens due to a dramatic change in the nature of the computation at late times. More specifically, the inspiralling compact object plunges into the central black hole and thus rapidly “disappears” from the computational domain, thereby transitioning the Teukolsky equation from one that is strongly source-term dominated, into its homogeneous form. This effect causes a modest change in the convergence rate of the code which ultimately reflects in the error plots depicted here.

*It is worth noting that these error levels are over an order-of-magnitude lower than those reported before [16].* The combination of our mathematical and computational advances have made this high-level of accuracy feasible.

### 5.2 Code Performance: Single GPU

Table 1 depicts the relative values for overall performance of our Teukolsky EMRI code for several variants of current generation CPUs and GPUs. These results suggest that it is relatively straightforward to obtain *order-of-magnitude* gains in overall code performance by making use of many-core GPUs over multi-core CPUs and this fact is largely independent of the specific hardware architecture and vendor. All the systems used in these performance tests used a variant of the Linux operating system and OpenCL provided by the appropriate vendor (AMD<sup>7</sup> or Nvidia<sup>8</sup>). Detailed specifications of the compute hardware are included in the table. The  $(r, \theta)$  grid size for this performance study is  $32000 \times 304$  that nearly utilizes the entire global memory capacity (3 GBs) of the considered GPUs. We use full *double-precision* floating point accuracy in all our computations. The emphasis on high-accuracy in this work requires us to make use of the highest grid resolution and numerical precision offered by the compute hardware.

It is also noteworthy that the consumer-grade GPU, the AMD Radeon HD 7970, outperforms Nvidia’s HPC-oriented,

<sup>7</sup>Catalyst 12.4; APP SDK 2.6

<sup>8</sup>CUDA 4.0

Name	Type	GHz	Cores	Perf.
AMD Opteron 6200	CPU	2.1	16	1x
Intel Xeon E5-2600	CPU	2.2	16	2.2x
Nvidia Fermi 2050	GPU	1.2	448	13x
AMD Radeon 7970	GPU	1.0	2000	19x

Table 1: This table depicts the relative values for overall performance for several variants of current generation CPUs and GPUs. The baseline system here has dual AMD Opteron, 8-core, 2.1 GHz CPUs running our OpenCL Teukolsky code. The remaining hardware listed above is co-located in a separate system.

high-end Fermi M2050 GPU, while maintaining a significantly lower cost<sup>9</sup>. The cost effectiveness of such consumer-grade compute hardware is nearly an order-of-magnitude higher than the alternatives. This observation is consistent with our earlier work that evaluated the *Sony PlayStation 3* consumer gaming console for scientific computing [13, 23].

### 5.3 Code Performance: Multiple GPUs

Figure 4 depicts the outcome of a strong scaling study performed on the XSEDE *Keeneland* system using our Teukolsky EMRI code. The message-passing based parallelization approach we take is explained in Section 4 of this article. The longer-duration EMRI computations scale much better, in particular the  $10^6 M$  long simulation scales almost perfectly. This is simply because, our parallel approach requires us to overlap the computations running on each GPU by a fixed amount, in order to perform the suitable “patching” during the post-processing stage. And because this overlap is of fixed duration, we start to receive diminished returns, especially for the cases with the larger number of GPUs. Of course, this overlapping is negligible for the very long duration cases, which is why the scaling is much better for those.

### 5.4 Science Enabled

In this section we document the current significant scientific contributions that have been made to the general area of gravitational physics (from gravitation wave physics to issues closely associated to Cosmic Censorship and also black hole astrophysics) owing to the development of our efficient and high-accuracy time-domain Teukolsky EMRI code.

1. *Waveform generation*: As pointed out in the previous sections, the advancements made to the TD Teukolsky EMRI code enable the code to perform very high accuracy and very long duration evolutions in a very efficient manner. As an example, in Ref. [6] we demonstrate relative errors in the gravitational wave energy flux at null infinity on the scale of  $10^{-4}$  and also perform a *million M* long EMRI evolution (over 10,000 orbital cycles – see Fig. 1).

<sup>9</sup>We are aware that with the release of the M2090 GPU, the M2050 is no longer the highest-grade Nvidia Fermi GPU anymore. However, we estimate that the Radeon 7970 would still outperform the M2090 on our tests.

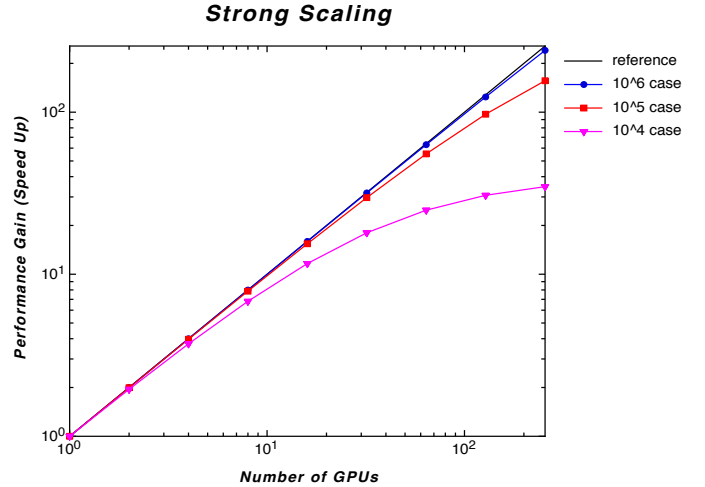


Figure 4: Strong scaling on the NSF XSEDE Keeneland supercomputer for several long-duration simulations.

2. *Calibration of EOB models*: Effective-one-body [15] formalism is an analytical approach that can very efficiently model black hole binary systems over a wide range of mass-ratios (from comparable to extreme) and is thus perhaps best suited for the generation of the large banks of templates needed for gravitational wave data analysis. High accuracy results from our code have contributed towards the development of a “calibrated” EOB model for large mass-ratio binaries with spin [16] in the context of quasi-circular, equatorial orbits.
3. *Recoil “kick” velocities*: Gravitational waves carry away linear momentum from a decaying binary, thus causing the system to recoil or “kick” [17]. A peculiar aspect of the recoil is that in certain scenarios (a prograde orbit decaying around a rapidly rotating black hole, in the context of large mass-ratios) there is a large “anti-kick” that appears very late in the plunge phase, that seems to completely cancel the large accumulated recoil present up to that point [5]. While there have been several mechanisms that have been proposed for this phenomenon, they all involve a significant role played by horizon perturbations i.e. quasi-normal ringing of the black hole. Recent work made possible due to the TD Teukolsky EMRI code suggests otherwise, and proposes a much simpler mechanism for the origin of the anti-kick [18]. In addition, as a by-product, the work also developed a scheme (“integration-from-peak”) using which one can obtain excellent estimates for kicks from very short evolutions, thus potentially being of great value to full NR.
4. *Cosmic Censorship*: It has been suggested multiple times in literature (see Ref. [19] for a recent proposal) that it may be possible for a near-extremal Kerr black hole to capture a test particle (on a specifically designed trajectory) that would result in overspinning the hole, thus forming a naked singularity in violation of the Cosmic Censorship Conjecture. The general expectation has been that once one accounts for

radiation-reaction, there would be no overspinning and therefore Cosmic Censorship would be preserved. We have now been able to demonstrate, through the use of the TD Teukolsky EMRI code, that it is actually the effect of the *conservative* part of the gravitational self-force that is likely responsible for preventing the overspinning [20, 21]. One way to describe the outcome of this research is that a near extremal Kerr hole simply fails to capture a test particle that could potentially overspin it!

## 6. CONCLUSIONS

In this article we demonstrate that recent mathematical and computational advances made to our time-domain Teukolsky EMRI code have enabled it to achieve a high-level of accuracy and efficiency. We emphasize the computational advancements made, that make use of the OpenCL framework to take advantage of the massive parallelism offered by modern many-core GPU architectures. The *order-of-magnitude* gain in computational performance we obtain in this manner plays a critical role in our code achieving the desired level of accuracy and efficiency.

The ability to perform high-accuracy and long-duration EMRI computations has enabled various interesting advances in gravitational physics. Using data generated by this code we have been able to make significant contributions to the development of effective-one-body models and gravitational waveform generation, that will ultimately positively impact the data analysis of current and future detectors (such as NSF’s LIGO and future space-borne missions). In addition, results from our code have brought forth a better understanding of the “anti-kick” which is an intriguing aspect of the phenomenon of gravitational recoil in decaying binary systems due to gravitational wave emission. And finally, our code has also helped test Cosmic Censorship in the context of the capture of a small test particle by a near extremal Kerr black hole.

## 7. ACKNOWLEDGMENTS

We would like to thank Mike DeSousa for double-checking several the accuracy level tests that we performed with the code. We are grateful to Glenn Volkema, Steve Liebling and Mark Barnell for providing useful feedback on an earlier version of this manuscript, and to the HPC group at MICROWAY for providing us access to some of the hardware we used in our study. We acknowledge research support from NSF Grant Nos. PHY-0902026, CNS-0959382, PHY-1016906 and PHY-1135664, and AFOSR DURIP Grant No. FA9550-10-1-0354 and also the Massachusetts Space Grant Consortium. Most of the numerical simulations needed for this work were performed on the NSF XSEDE *Keeneland* supercomputer under project number UT-NTNL0036.

## 8. REFERENCES

- [1] R. Lopez-Aleman, G. Khanna and J. Pullin: “Perturbative evolution of particle orbits around Kerr black holes: time domain calculation”, *Class. Quantum Grav.* **20**, 3259 (2003).
- [2] L. M. Burko and G. Khanna: “Accurate time-domain gravitational waveforms for extreme-mass-ratio binaries”, *Europhys. Lett.* **78**, 60005 (2007).
- [3] P. A. Sundararajan, G. Khanna, and S. A. Hughes: “Towards adiabatic waveforms for inspiral into Kerr black holes: I. A new model of the source for the time domain perturbation equation”, *Phys. Rev. D* **76**, 104005 (2007).
- [4] P. A. Sundararajan, G. Khanna, S. A. Hughes, S. Drasco: “Towards adiabatic waveforms for inspiral into Kerr black holes: II. Dynamical sources and generic orbits”, *Phys. Rev. D* **78**, 024022 (2008).
- [5] P. A. Sundararajan, G. Khanna, S. A. Hughes: “Binary black hole merger gravitational waves and recoil in the large mass ratio limit”, *Phys. Rev. D* **81**, 104009 (2010).
- [6] A. Zenginoglu, G. Khanna: “Null infinity waveforms from extreme-mass-ratio inspirals in Kerr spacetime”, *Phys. Rev. X* **1**, 021017 (2011).
- [7] S. Teukolsky: “Perturbations of a rotating black hole”, *Astrophys. J.* **185** 635 (1973).
- [8] W. Krivan, P. Laguna, P. Papadopoulos, and N. Andersson: “Dynamics of perturbations of rotating black holes”, *Phys. Rev. D* **56**, 3395 (1997).
- [9] Nvidia’s CUDA <http://www.nvidia.com/cuda/>
- [10] AMD’s Stream <http://www.amd.com/stream>
- [11] OpenMP <http://openmp.org>
- [12] Khronos OpenCL <http://www.khronos.org/opencl/>
- [13] G. Khanna, J. McKennon: “Numerical modeling of gravitational wave sources accelerated by OpenCL”, *Computer Physics Communications* **181**, 1549 (2010).
- [14] N. Choudhary, R. Gajopalli, S. Navada and G. Khanna: “An Exploration of OpenCL for a Numerical Relativity Application”, *Proceedings of the Parallel and Distributed Computing Systems (PDCS) conference*, Dallas, TX (2011).
- [15] A. Buonanno and T. Damour: “Effective one-body approach to general relativistic two-body dynamics”, *Phys. Rev. D* **59**, 084006 (1999).
- [16] E. Barausse, A. Buonanno, S. A. Hughes, G. Khanna, S. O’Sullivan and Y. Pan: “Modeling multipolar gravitational-wave emission from small mass-ratio mergers”, *Phys. Rev. D* **85**, 024046 (2012).
- [17] M. Favata, S. A. Hughes, D. Holz: “How black holes get their kicks: Gravitational radiation recoil revisited”, *Astrophys. J.* **607**, L5 (2004).
- [18] R. H. Price, G. Khanna and S. A. Hughes: “Systematics of black hole binary inspiral kicks and the slowness approximation”, *Phys. Rev. D* **83**, 124002 (2011).
- [19] T. Jacobson and T. Sotiriou: “Overspinning a Black Hole with a Test Body”, *Phys. Rev. Lett.* **103**, 141101 (2009).
- [20] E. Barausse, V. Cardoso and G. Khanna: “Test bodies and naked singularities: is the self-force the cosmic censor?”, *Phys. Rev. Lett.* **105**, 261102 (2010).
- [21] E. Barausse, V. Cardoso and G. Khanna: “Testing the Cosmic Censorship Conjecture with point particles: the effect of radiation reaction and the self-force”, *Phys. Rev. D* **84**, 104006 (2011).
- [22] S. Field, J. Hesthaven, S. Lau: “Persistent junk solutions in time-domain modeling of extreme mass ratio binaries”, *preprint arXiv:1001.2578* (2010).
- [23] PS3 Gravity Grid <http://gravity.phy.umassd.edu/ps3.html>